SMAR 2019 – Fifth Conference on Smart Monitoring,
Assessment and Rehabilitation of Civil Structures

SMAR 2019

Numerical Modelling of Corroded Reinforced Concrete Beams Based on Visual Inspection Data

Hussein NASSER [1], Charlotte VAN STEEN [1], Rutger VRIJDAGHS [1], Andrés A. TORRES-ACOSTA [2], Lucie VANDEWALLE [1], Els VERSTRYNGE [1]

[1] KU Leuven, Leuven, Belgium

[2] Universidad Marista de Querétaro, Querétaro, Mexico

Contact e-mail: hussein.nasser@kuleuven.be

ABSTRACT: Chloride-induced corrosion in existing reinforced concrete structures remains a main issue for structural engineers. It is a challenge to predict the structural effects of the deteriorations due to corrosion, such as formation of pits in the rebar, cracking of the concrete cover and the loss of bond strength. Recent research on corrosion damage has mainly focused on the following four aspects; inspection techniques and condition assessment, micro-modelling of the corrosion process, empirical damage relations and macro-modelling of the behaviour of corroded beams based on experimental data. Although the models in literature provide good predictions in comparison with experiments, they are mostly based on the exact value of mass loss that is quantified after extracting the bar from the beam. However, the mass loss is a quantity that is not exactly known from on-site inspection. Therefore, the following paper proposes a novel modelling framework that links visual inspection data to a 2D numerical model. The aim is to study the efficiency of a 2D modelling approach in predicting the behaviour of corroded RC beams by using damage relations that are based on visual inspection data. Simulating the inspection-based study is based on the experimental data of a test program with reported crack widths. The findings of the paper report on the accuracy of the inspection-based methodology within a deterministic framework, the efficiency of the adopted damage relations as well as the efficiency of updating a 2D beam model to predict the structural behaviour of corroded beams based on crack width measurements.

1 INTRODUCTION

Deteriorating reinforced concrete structures due to chloride-induced corrosion are a major concern for the construction industry nowadays. Different inspection tools are used to assess these deteriorations. Firstly, visual inspection is performed. During the visual survey, location of rust spots, concrete cover cracks and exposed reinforcement are determined. Moreover, crack widths can be measured with a crack meter. Secondly, detailed inspection is performed in order to quantify the severity of the corrosion damage. For this purpose, covermeters are used to locate the reinforcement, determine the diameter of the bars and the cover depth. Furthermore, Galvapulse can give both qualitative and quantitative inspection results as shown in Andrade et al. (2001) where resistivity and the corrosion potential give an indication of the active zones of corrosion while the corrosion rate can be transformed into section loss through Faraday's law. Yet, since the corrosion process in not constant in time and on-site conditions affect the these measurements, care should be taken interpreting the results.

Inspection surveys provide a good understanding of the severity of the chloride-induced damage according to which the structural component can be classified into different levels of corrosion as

in Contecvet (2001). These classifications provide an important method for the assessment of the condition of the structure; however, less is known about the remaining structural capacity of the reinforced concrete (RC) component. Since numerical tools provide a good prediction of the structural behaviour of concrete structures, incorporating the inspection-data into a numerical structural model can assist in the prediction of the structural behaviour of RC structures with chloride-induced corrosion damage. Therefore, this paper focuses on using information of corrosion crack width as an input to predict the behaviour of RC beams by numerical modelling.

2 INTERPRETATION OF CORROSION INSPECTION DATA

The nature of the chloride-induced corrosion mechanism causes damage on the level of rebar, concrete cover and the steel-concrete interface. First, local cross-section loss occurs due to the formation of pits along the rebar. Secondly, the concrete cover cracks due to the expansive nature of the corrosion products which eventually leads to spalling and the exposure of the corroded rebar. Moreover, integrity between the concrete and the steel bar which is ensured by bond mechanism is lost. By quantifying the different deteriorations, the effect of corrosion damage can be determined which assists in the assessment of the structural capacity of the RC structural component.

Condition assessment is based on using inspection data to determine the level of corrosion damage. The Contecvet report classified four levels of corrosion based on six indicators: carbonation depth, chloride level, corrosion crack width, rebar section loss, resistivity and corrosion rate. It also suggests indices which assist with the assessment and the decisions regarding the urgency of intervention. Other authors, such as Shimomura et al. (2011), provided a different type of classification which is only based on qualitative visual inspection of the state of the component. These classifications provide a good initial understanding of the state of the structure however, to develop a numerical model, information of material and section properties are needed. Because corrosion-induced concrete cracking is visible on the surface and measuring the section loss of the corroded rebar is a challenge, several authors showed correlations between crack width (w) and section loss (ΔA) or penetration depth (x) which can be applied in an inspection-based numerical modelling framework (Table 1).

Table 1. Different reported damage functions

Author	Damage relationship		
Torres-Acosta et al. (2007)	$w=6{,}4\left(\frac{x}{r_0}\right)^{0{,}82}$	(1)	r_0: initial rebar radius (mm)
Rodríguez et al. (2006)	$w=0{,}05+\beta(x-r_0)$	(2)	β: factor depending on the bar position
Khan et al. (2014)	$w=0{,}1916\frac{\varphi}{c}\Delta A+0{,}164$	(3)	φ: rebar diameter (mm)
			c: cover depth (mm)

3 THE EXPERIMENTAL PROGRAM BY A.TORRES-ACOSTA ET AL (2007)

In order to simulate the inspection-based approach, the data of an experimental program with reported corrosion crack widths is used. This serves to validate the approach of using empirical relations relating the inspected crack width to the mass loss. It is worth mentioning, that the relation is based on accelerated corrosion experiments which can differ from what is encountered under natural conditions. Therefore, the paper focuses on the modelling approach rather than on generalizing the empirical relation from these experiments.

3.1 Overview of test campaign and results

The experimental campaign by Torres-Acosta et al. (2007) studied the flexural behaviour of a reinforced concrete beam with one tension rebar as a function of four different corrosion levels; no corrosion 0%, low corrosion 5%, medium corrosion 10 % and high corrosion 15%. The beam had dimensions of 1500x150x100 mm and were reinforced with a #3 rebar which corresponds to a diameter of 9.5 mm and a cross-section area of 71 mm^2. The cover depth was 2 cm. Twelve beams were cast with the average concrete strength at 28 days being 27 MPa. Four of these beams (B01, B02, B11 and B12) were non-corroded and acted as control beams while the remaining eight beams were corroded to the different levels. In order to accelerate the corrosion process, the author added 3% NaCl salt by weight of cement to the concrete mixture. A current density of 80 $\mu A/cm^2$ circulated from a steel plate glued to the side of the beam (cathode) to the steel rebar (anode). After the corrosion process finished, the beams were subjected to a three-point bending test which provided load deflection curves. The results of the experimental program are shown in Table 2 where the percentage reduction is calculated relative to the average yield load of the three control beams (11.40 kN).

Table 2. Results of corrosion damage measurements as reported by A.Torres-Acosta et al (2007)

Beam	Radius loss (%)	Mass loss (%)	Maximum crack Width (mm)	Maximum pit depth (mm)	Failure mode	Yield load (kN)	Reduction in load (%)
B01	-	-	-	-	Yielding	11.00	-
B02	-	-	-	-	Yielding	12.10	-
B03	5.10	10.30	0.5	3.35	Yielding	7.50	34.21 %
B04	8.80	17.70	1.25	6.20	Yielding/Rupture	4.30	62.28 %
B05	9.20	18.40	0.50	7.03	Yielding/Rupture	4.50	60.53 %
B06	6.00	12.00	3.00	2.54	Yielding	7.90	30.70 %
B07	5.40	10.80	0.60	3.39	Yielding	7.50	34.21 %
B08	10.60	21.30	1.50	4.38	Yielding	7.10	37.72 %
B09	9.70	19.50	1.50	3.84	Yielding	6.50	42.98 %
B10	16.10	32.20	1.70	7.40	Yielding/Rupture	3.10	72.81 %
B11	Broken during handling as reported in Torres-Acosta et al. (2007)						
B12	-	-	-	-	Yielding	11.10	-

3.2 Interpretation of the experimental data

The classification of the beams is based on visual inspection data which is provided in the form of the maximum crack width of the longitudinal crack which is assumed to be representative. The classes are adapted from Contecvet (2001), see Table 3, where a limit of 1.5 mm is inserted between the medium and high corrosion level. Moreover, beam B06 is omitted from the classification and the modelling since it is reported to have developed an unusually wide crack while the mass loss was still low. With the limited damage and material property data available, it is not possible to explain the experimental results of beam B06.

Table 3. Condition Assessment of the different beams according to the maximum crack width

Corrosion damage level	Crack width (mm)	Beams
No corrosion	No cracking	B01 B02 B11 B12
Low	< 0.3	None
Medium	[0.3-1.5[	B03 B04 B05 B07
High	≥1.5 and/or major spalling	B08 B09 B10

The empirical damage relation by Khan et al. (2014) incorporates the rebar diameter and the cover depth as parameters influencing the crack formation, therefore it will be used as a relation to

predict the mass loss based on crack width data of the experimental program (Figure 1). As shown in Table 4, the error in prediction by using this relation is observed to be high for the case of B05 and B10. This can be attributed to the stochastic nature of the corrosion process and concrete cracking.

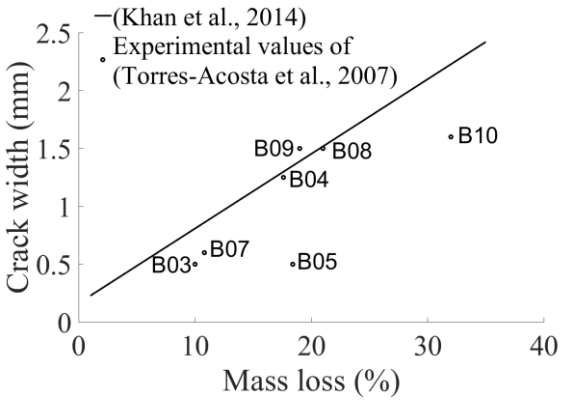

Figure 1. Damage functions relating the crack width to the mass loss of the steel rebar.

Table 4. Error in prediction on rebar cross-section

Beam	Maximum crack width (mm)	Measured section loss (%)	Predicted section loss (%)	Error (%)
B03	0.50	10.30	5.20	5.60
B04 (deep pit)	1.25	17.70	16.80	1.00
B05 (deep pit)	0.50	18.40	5.20	16.20
B07	0.60	10.80	6.80	4.60
B08	1.50	21.30	20.70	0.70
B09	1.50	19.50	20.70	1.60
B10 (deep pit)	1.70	32.20	23.80	12.40

4 MODELLING OF CORROSION DAMAGE

The structural behaviour of the beams is modelled through a 2D longitudinal beam model developed in DIANA 10.2. This type of model takes into account the steel cross-section, bond-slip behaviour as well as the concrete properties which allows to apply reduction factors as a function of the measured corrosion damage without the need of modelling the corrosion process at the micro-scale (Michel et al. (2016)).

4.1 Model Description

The model is discretized by a mesh of size 10 mm using quadrilateral elements where the steel is modelled as a bond-slip truss element with its centreline positioned at 24.75 cm from the bottom of the beam to account for the cover depth. The concrete and steel material properties are summarized in Table 5. The calculation of the concrete material properties is based on the formulas of fib (2010) as a function of the compressive strength except for the compression fracture energy (G_c) which is calculated according to Nakamura et al. (1999) by $G_c=250G_f$ where G_f is the tensile fracture energy.

However, the beams of the experimental program show higher deflection values to what is expected from a rigid RC beam. This can be attributed to either pre-cracking during curing and/or corrosion or local crushing and settlement of the beams at the supports or lack of rigidity of the testing frame which resulted in an increase in the measured deflections. For the present paper, the pre-cracking is assumed which affects the stiffness of the member and it is reflected by calibrating

the cracked concrete properties as shown in Table 5 until the numerical results agree with the results of the reference beams. The non-linear analysis in DIANA is based on a smeared total strain rotating crack model. A displacement-based Newton-Raphson iteration procedure is used with load steps of 0.1. Convergence is based on energy and force norms both of which is defined as 0.01 and a maximum of 250 iterations is defined.

Table 5. Material properties and models used in DIANA 10.2

Concrete material properties		Adapted properties	Steel material properties	
E_c (GPa)	29.60	3.80	E_s (GPa)	210.00
ν	0.20	0.20	ν	0.30
f_{cm} (MPa)	27.00	27.00	f_y (MPa)	412.00
G_c (N/mm)	33.00	33.00	f_u (MPa)	625.00
f_t (MPa)	2.14	1.50	ε_u (%)	10.00
G_f (N/mm)	0.13	0.40	Plasticity model	Von Mises
Tension softening	Hordijk		Bond-slip model	fib 2010
Compression softening	Parabolic			

4.2 Damage functions

The corrosion damage is translated to the numerical model as reduction factors on the section and material properties for both concrete and steel. For this reason, different formulas are used to apply these reductions as a function of the rebar cross-section loss.

The steel section loss is estimated as the average section loss per corrosion level. Regarding the beams that failed by rupture, the spherical pit model by Val et al. (1997) is used in addition to applying the average section loss. The pit length (L_{pit}) is taken the same as the pit width in the Val et al. (1997) pit model. Finally, the altered yielding and ultimate tensile strengths (f') as well as the ultimate strain (ε_u) of the steel are calculated as a function of the section loss (ΔA(%)) according to the formulas of Imperatore et al. (2017), equations (4) and (5). The value of α is 0.019 for the yield strength while it is 0.018 for the ultimate strength.

$$f' = (1 - \alpha \Delta A) f \quad (4) \qquad \varepsilon_u = e^{-0{,}054 \Delta A} \quad (5)$$

Cracking of the concrete cover is modelled by reducing the tensile strength of the concrete cover according to the approach used by Coronelli et al. (2004). First, the compressive strength is reduced according to equation (6) which considers the maximum strain reached by the concrete ($\varepsilon_o = 0.2\%$) and the increase in strain due to crack formation which is calculated, according to equation (7), as a function of the crack width (w_{cr}), number of bars (n_{bars}) and initial width of the beam section (b_0). Finally, the tensile strength of the cracked cover is determined according to equation (8).

$$f_{cm}^{cracked} = \frac{f_{cm}}{1+0.1\frac{\varepsilon_1}{\varepsilon_o}} \quad (6) \qquad \varepsilon_1 = \frac{b_f - b_0}{b_0} = \frac{n_{bars} w_{cr}}{b_0} \quad (7) \qquad f_t^{cracked} = \frac{f_{cm}^{cracked}}{f_{cm}} f_t \quad (8)$$

Bond deterioration is modelled by adopting a splitting bond failure mode (Figure 2) which reduces the maximum bond strength and the maximum slip. For this paper, the pull-out failure of the bond is modelled according to fib (2010) while, for the splitting bond failure, the damage model of Rao (2014), equation (9) , is used to reduce the maximum bond strength. Then, this value is used to calculate the slip value at which the maximum bond strength is reached. Furthermore, to adopt a splitting bond failure, the slip value (s_2) from the fib bond model is set equal to the slip value (s_1).

$$\begin{cases} \tau = \tau_{max} & \text{for } \Delta A < 2\% \\ \tau = 1.5\tau_{max} \Delta A^{-0.6} & \text{for } \Delta A > 2\% \end{cases} \quad (9)$$

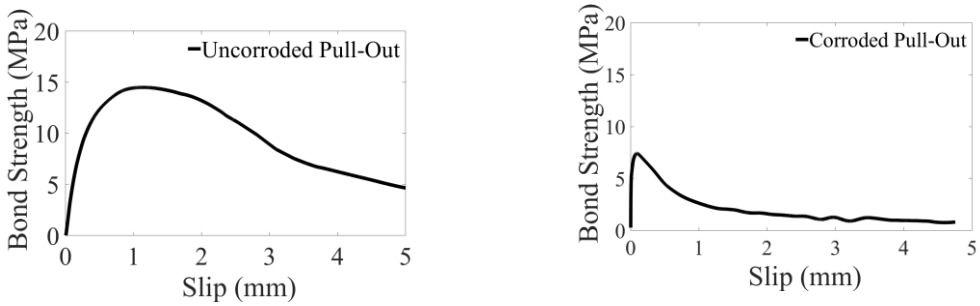

Figure 2. Pull-out bond failure of an uncorroded rebar (left), splitting bond failure of a corroded bar (right) Van Steen et al. (2019).

5 RESULTS

The numerical modelling results are represented in Figure 3 which shows three shaded zones representing the different corrosion levels. The area of each zone is the area between the experimental curves of the beams that are classified to be of the same corrosion level.

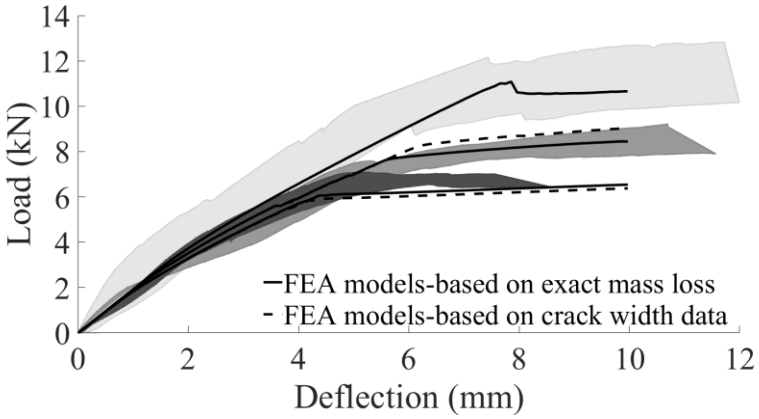

Figure 3. Experimental and numerical load deflection curves for different corrosion levels, from top to bottom, no corrosion, medium corrosion and high corrosion.

Two approaches are used to calculate the rebar section loss for each corrosion level. In a first approach, the section loss is calculated based on the gravimetric results while the second approach estimates the section loss from the crack width according to equation (3). It has been observed from the modelling that the bond reduction had no effect on the behaviour of the beam regarding the stiffness or the yield load. It has also been noticed that the reduction in the tensile strength and the tensile fracture energy of the concrete cover due to the corrosion crack is responsible for the reduction in stiffness and further reduction in the yield load. The tensile fracture energy has been calibrated until a good agreement with the experimental results is achieved.

5.1 Results based on destructive evaluation of rebar mass loss (real mass loss)

Table 6. Experimental and numerical results based on measured section loss

Corrosion level	Average measured residual section (mm^2)	Average experimental yield load (kN)	Numerical prediction (kN)	Modelling error (%)
Medium	63.40	7.50	7.60	1.30
High	56.45	6.80	6.00	11.70

The results of this approach are summarized in Table 6. A good agreement is achieved between the experimental and numerical results regarding the stiffness reductions of the corroded beams, as shown in Figure 3. Regarding the yield capacity of the beams, a good agreement can also be observed especially for the medium corrosion level where the modelling error is 1.30 %. The high corrosion level, however, shows an error of 11.70 % .

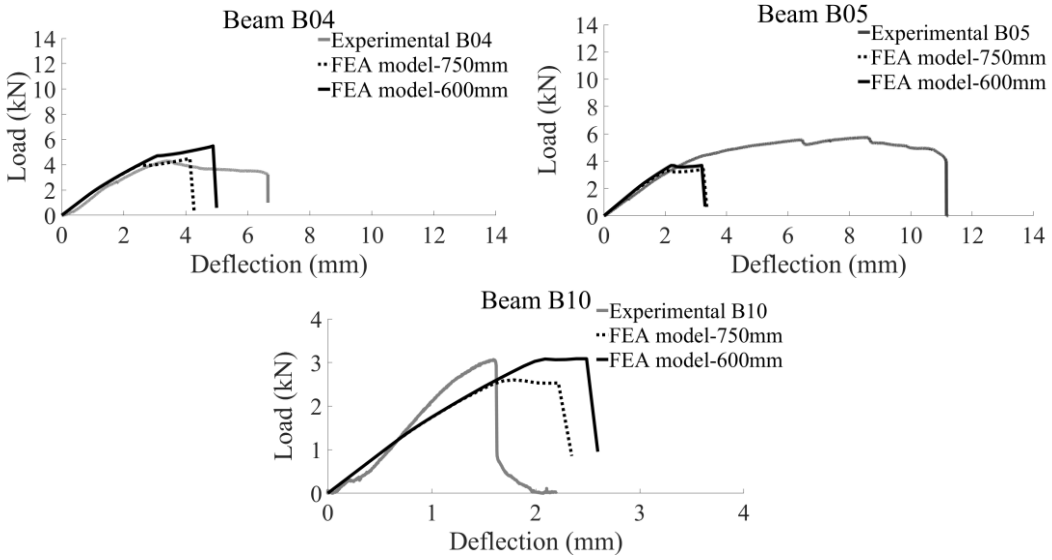

Figure 4. Load deflection curves of B04, B05 and B10.

Three beams are reported to show failure due to rupture at the location of the deepest pit. Therefore, the pit is modelled as a separate reinforcement truss element of length L_{pit} and cross-section corresponding to the section of spherical pit model. Because the location of the deepest pit is not reported, two different positions are considered in the model: one at 750 mm and another at 600 mm from the edge of the beam. Numerical results of beams B04 and B10 (Figure 4) show a good agreement with the experimental behaviour regarding both the stiffness, failure mode and load level. However, the experimental curve of B05 shows a more ductile behaviour which is not observed in the numerical result nor in the experimental data of beams B04 and B10. Finally, the results show that the yield load is less reduced as the pit location is further away from the position of maximum moment.

5.2 Results based on estimating the rebar mass loss by using crack width data

Table 7. Results of numerical modelling using crack width data

Corrosion level	Average predicted residual section (mm^2)	Average experimental yield load (kN)	Numerical prediction based on crack width (kN)	Modelling error (%)
Medium	66.50	7.50	8.10	8.00
High	56.00	6.80	5.80	14.70

As a second approach, after having a validated numerical model, the section loss is recalculated by using the crack width and the relation of Khan et al. (2014). By using the new value of the section loss, the reduction parameters (steel material properties and bond loss) while those that are related to the crack width (concrete tensile strength and fracture energy) are kept the same as in the previous section. It can be observed from the load-deflection curves in Figure 3 that a slight difference in the trend occurs which is attributed to the error in prediction of the damage model. The damage model predicts the mass loss of the medium corrosion level with an error of 4.8% while the error in prediction for the high corrosion level is 0.8%. By comparing the experimental

yield load to that of the numerical, it can be seen that an error of 4.8% and 0.8 % on the section loss causes an increase of 6.70% and 3.00% in the modelling error for the medium and high corrosion, respectively.

6 CONCLUSION

The presented research investigated the prediction of the structural capacity of corroded reinforced concrete beams based on crack width data. Modelling the damage using reduction factors for the material and section properties in a 2D longitudinal beam model is efficient in reproducing the structural behaviour. Moreover, this modelling approach can be coupled with empirical relations which relate the corrosion crack width to the section loss of the rebar or pit locations. Although such approach has the advantage that structural capacity of the degraded RC beams can be reliably estimated from inspection data, the applied empirical relations are dependent on the RC component's layout and parameters of the corrosion process. Therefore, the development of more universal, inspection-based damage relations and an inclusion of the stochastic nature of the involved processes are vital in further research.

7 ACKNOWLEDGMENT

The authors would like to thank the internal funds of KU Leuven for supporting the following research which is in the framework of the C24/14/042 project “Multi-scale assessment of residual capacity of reinforced concrete structures”

8 REFERENCES

Andrade, C. and Alonso, C., 2001, On-site measurements of corrosion rate of reinforcements. Construction and Building Materials, 15(2-3): 141-145.

Contecvet, 2001, CONTECVET, A validated users manual for assessing the residual life of concrete structures-Manual for assessing corrosion-affected concrete structures.

Coronelli, D. and Gambarova, P., 2004, Structural Assessment of Corroded Reinforced Concrete Beams: Modeling Guidelines. Journal of Structural Engineering, 130(8): 1214-1224.

fib, 2010, fib Model Code for Concrete Structures.

Imperatore, S., Rinaldi, Z. and Drago, C., 2017, Degradation relationships for the mechanical properties of corroded steel rebars. Construction and Building Materials, 148(2017): 219-230.

Khan, I., François, R. and Castel, A., 2014, Prediction of reinforcement corrosion using corrosion induced cracks width in corroded reinforced concrete beams. Cement and Concrete Research, 56(2014): 84-96.

Michel, A., Lepech, M., Stang, H. and Geiker, M., 2016, Multi-physical and multi-scale deterioration modelling of reinforced concrete: modelling corrosion-induced concrete damage, 9th International Conference on Fracture Mechanics of Concrete and Concrete Structures, Berkley, California.

Nakamura, H. and Higai, T., 1999, Compressive Fracture Energy and Fracture Zone Length of Concrete, Modelling of Inelastic Behaviour of RC Structures, Tokyo-Japan.

Rao, A. S., 2014, Structural Deterioration and Time-Dependent Seismic Risk Analysis, PhD Thesis, Civil and Environmental Engineering, Stanford University, Stanford.

Rodríguez, J., Ortega, L., Izquierdo, D. and Andrade, C., 2006, Calculation of structural degredation due to corrosion of reinforcements, Measuring, Monitoring and Modeling Concrete Properties, Dordrecht.

Torres-Acosta, A., Navarro-Gutierrez, S. and Terán-Guillén, J., 2007, Residual flexure capacity of corroded reinforced concrete beams. Engineering Structures, 29(6): 1145-1152.

Val, D. and Melchers, R., 1997, Reliability of Deteriorated RC Slab Bridges. Journal of Structural Engineering, 123(12): 1638-1644.

Van Steen, C., Verstrynge, E., Wevers, M. and Vandewalle, L., 2019, Assessing the bond behaviour of corroded smooth and ribbed rebars with acoustic emission monitoring. Cement and Concrete Research, 120(2019): 176-186.